Vacuum microelectronics: application perspectives for future display technology

M.A. HERMAN

Research and Development Centre of Vacuum Electronics OBREP,
Długa 44/50, 00-241 Warszawa, and

Institute of Physics, Polish Academy of Sciences, Lotników 46,
02-668 Warszawa, Poland

1. Introduction

For many years, the designers of electronic systems have thought almost exclusively about the use of semiconductor devices. The vacuum tube, once the main-stay of electronics, has always carried the heritage of its early design, with a glass envelope preventing miniaturization and integration, and the thermionic cathode keeping the power drain high. Recent developments offer the opportunity to break away from these restraints. Semiconductor lithography can be used to machine shapes that develop high fields from relatively low voltages, thus giving a cold electron emitter. The cathode-anode spacing can be very small (20–50 μm) permitting the integration of many devices on a small chip.

The possibility of producing devices that are capable of withstanding high-voltage stresses and are also able to work at high and variable temperatures offers an enticing new generation of electronic devices. Not limited by electron-phonon scattering, the high speed associated with these components can give terahertz switches. Stabilization and control of the cold cathode emission will be a key factor in determining the success of this new field, which promises many novel applications.

The name Vacuum Microelectronics (VM) was introduced for this field in 1988, at the 1st International Conference in Williamsburg Virginia, USA [1]. Since then, conferences on VM have been held annually [2–4]. The fifth meeting took place in Vienna, Austria, August 1992.

VM was developed mainly during the 1980s. Considerable interest were raised in 1986, when a planar vacuum field effect transistor was successfully demonstrated by Gray et. al. [5]. VM is based largely on the utilization of field emission and cold cathode electron sources which are microengineered to be used in electron beam displays, vacuum microvalves, speciality sensors, and interfaces with microelectromechanical devices [6]. This technology originated in the semiconductor industry and today shows great promise for devices and systems used in special applications (space exploration systems, microrobots, high temperature microelectronic devices, etc.).

Integrated VM circuits with field emission cathodes can provide advantages over common, silicon, integrated-circuits in specialized applications. The quantum mechanical tunneling inherent in the field emission process is relatively insensitive to temperature and ionizing or particle irradiation. Potentially, the device can operate at very high voltage levels, since reverse-biased *p-n* junctions need not be present in the circuit. The device designs may operate in nanowatt and picowatt power ranges. At sufficiently high current density and power dissipation, the VM device is capable of a maximum frequency of operation higher than semiconductor devices because there is no mobility saturation for the electron trajectory in a vacuum.

In essence a VM system envisages the application of silicon micro-engineering techniques [7] to fabricate micro-sized arrays of old fashioned vacuum tube devices such as diodes, triodes, pentodes, etc. [2, 3].

The major challenge of this new technology is therefore to develop a micro-electron source that exhibits long-term stability, that can be replicated with high surface densities, and consumes only minimal power. To meet these requirements, one is almost bound to use some form of field, or „cold", emission electron source, and so it is not surprising that much of the current effort is being concentrated on fabricating arrays of etched Si [8] or Mo [9] micro-emitters.

2. *Field emitter arrays*

Field emitter arrays (FMAs), are the key element in VM technology. FMAs are multiple arrays of electron emitters, each of which is controlled by a gate electrode. Fig. 1 shows a cross section, and Fig. 2 shows a SEM micrograph of one element of a Spindt-type array cathode [9]. A SEM micrograph of a matrix of arrays of Spindt-type field emitters is shown in Fig. 3 [10].

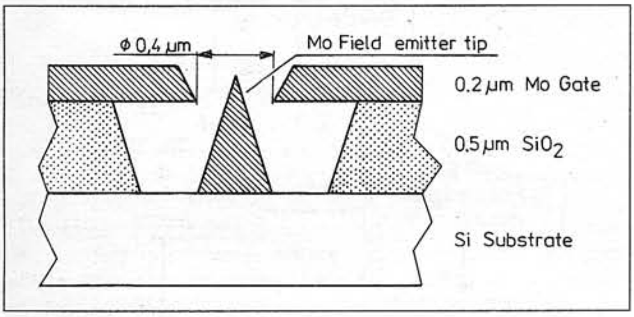

Fig. 1. Cross section of one element of an array cathode (from Ref. [9])

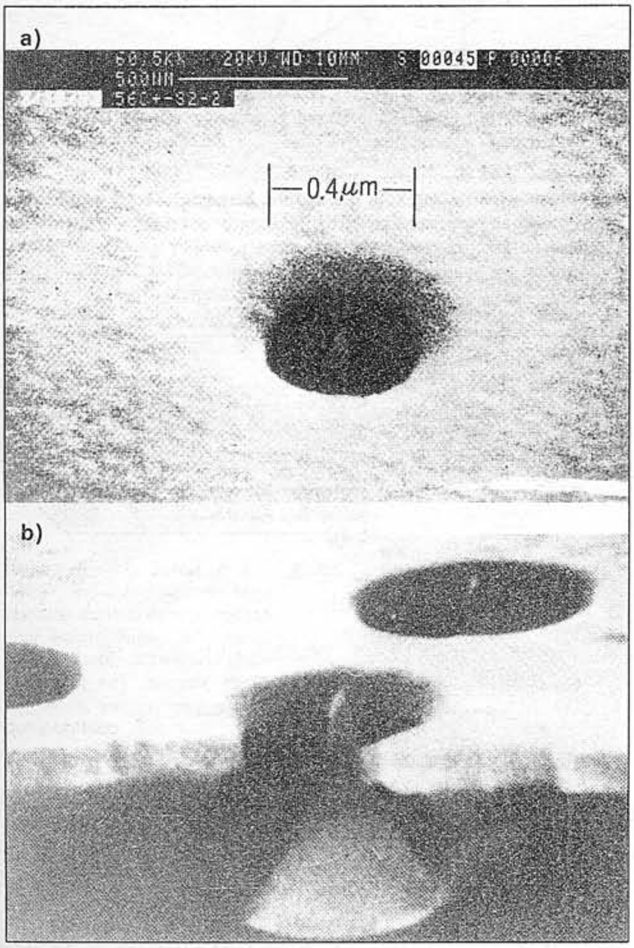

Fig. 2. SEM micrograph of one gated field emitter: a) from Ref. [9], b) from Ref. [10]

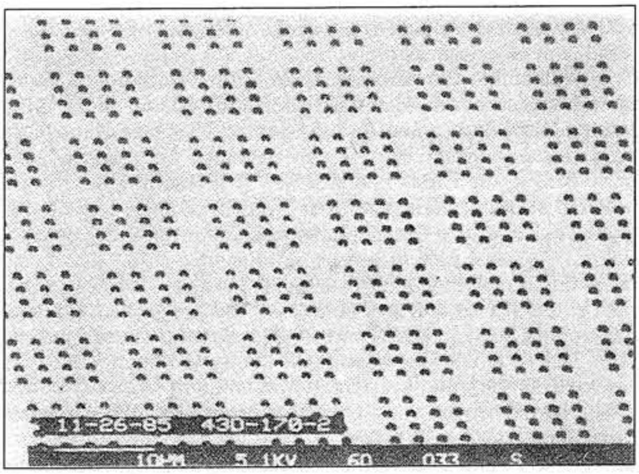

Fig. 3. SEM micrograph of Spindt cathode array for vacuum microelectronics applications (from Ref. [10])

When a positive potential difference is applied between the substrate and the gate of a field emitter, an electric field is generated at the tip that allows electrons to tunnel from inside the metal to the vacuum outside, when the field exceeds about 5×10^7 V/cm. The field at the tip and, thus, the quantity of electrons emitted are controlled by the gate potential. Field emission is the most practical method of injecting the electrons into the vacuum. This is caused by the physical attributes of the field-emission process [11]:

- The very high-current densities necessary to obtain a measurable number of electrons in a short period of time from a source of a very small area are only obtainable with field emission. For example, 1000 electrons in 10^{-12} s from an area of 10^{-10} cm^2 corresponds to a current density of 1.6×10^6 A/cm^2.
- Quantum mechanical tunneling requires zero power to transfer electrons into the vacuum.
- Field-emission sources are not as dependent on the crystalline state and perfection of the emitter material as is the case with solid-state devices.

The theoretical basic of field emission is usually described by the Fowler-Nordheim equation [12].

$$J = 1.54 \times 10^{-6} \frac{E^2}{\varphi t^2(y)} \exp\left[-6.83 \times 10^7 \frac{\varphi^{3/2}}{E} f(y)\right] \quad (1)$$

Where J is the current density in A/cm^2, φ is the work function of the emitter in eV. E is the electric field in V/cm. The functions $f(y)$ and $t(y)$ have been calculated to be 1, approximately [11]. Therefore, one may use the following simple expresion of equation (1)

$$\frac{I}{V^2} = a \exp\left[-\frac{b}{\beta V}\right] \quad (2)$$

Where a and b are constants, and $E = \beta V$, V is the voltage across the cathode tip and anode, β is the local field conversion factor at the emitting surface, determined by the structure of tip and distance between tip and anode. The field at the apex of the tip is inversely proportional to the tip radius. This is the reason why sharp needle structure tips are fabricated to achieve the requirement for high electric field which yields reasonable field emission current [13].

Densely packed arrays of microfabricated field emitters (> 10,000,000 tips per sq.cm) with integrated-extractor or gate electrodes have been shown to produce 100's of A/cm^2 of emission current with very high efficiencies [9]. For most applications, it is desirable for the emitter array to have as low an operating voltage as possible. Therefore, the smallest size of the apertures in the extraction or gate electrode that can be consistently patterned in order to reduce the operating voltage is a very important issue in the fabrication of Spindt-type field emitter arrays [14]. The diameter of these apertures should be less than 0.5 μm in order to obtain field emission well below the

100 V operating voltage and the apertures must be manufactured with an extremely high uniformity. 5 : 1 optical lithography is well suited to manufacture thousands of identical apertures because of the low pass behaviour of the optics with respect to the high spatial frequencies, and because of the high precision with which reticles can be made. Lithography was performed in the experiments of Ref. [9], resulting in circular holes of about 1 μm in the resist layer. In order to reduce the aperture diameter in the molybdenum gate layer to the desired 0.4 μm the resist pattern has been transferred into a sacrificial layer on top of the gate layer by reactive ion etching. The deposition of a second sacrificial layer and subsequent reactive ion etching leads to a well controlled reduction of the aperture size. The field emission tips have been manufactured using Spindt's self aligning evaporation technique [14].

The current density delivered by present FEAs [9] has been demonstrated up to 1000 A/cm^2. It will not be a great surprise to obtain 10^4 A/cm^2 after further downsizing and higher packing density.

The operating gate voltage has been brought down to $\approx$ 50 V and can be further reduced to the level of LCDs in the not too distant future. Because of tunneling, instead of thermionic electron emission, the output current responds to the gate voltage instantly which implies that no energy is required for electron emission in a static case. In suitable geometric configurations, the current collected by the gate can be as low as 0.1% of the total emission current.

In addition to all of the excellent characteristics, mentioned above, the most dramatic advantage of FEAs against all other field emission devices of the past is the fact that FEAs can be operated in vacuum environments of 10^{-6} Torr, and the lifetime of these emitters can be > 10.000 hrs. under sealed tube conditions. There is no requirement for ultra-high vacuum for durable field emission. This is due to the special field configuration of FEAs which automatically prevent bombardment of the emitter surfaces by ions which are formed by electron impact ionization in space as well as on anode surfaces. This fundamental but unique property of FEAs has made possible industrial applications for field emission phenomena for the first time.

Therefore, it is not surprising that many groups want to use FEAs to make the ultimate Flat Panel Displays (FPDs) which are characterized by high brightness, high definition, multi-colored, do not need backlighting, have low power consumption, and are suitable for large size and good manufacturability. As far as manufacturability is concerned, FPDs based on FEAs will in principle give high production yields due to the high redundancy inherent in FEAs, namely multiple emitters per pixel.

For screen sizes, one may expect that the most appropriate size for FEAs based FPDs for HDTV application is in the range of 50 inch $\approx$ 100 inch diagonals.

A flat fluorescent display of this type has been demonstrated by Meyer et al. already in 1986 [15]. It was based on a matriced array of cold cathode emitters. Each pixel was addressed by several thousands of electron microguns. This low power (1 W/dm^2) and highly efficient (1–10 lm/W) device allows basically full color rendering with high resolution and brightness.

3. Modelling of the field emission flat panel display performance

In 1990 Meyer demonstrated the feasibility of FEA based flat panel displays (FPDs) with a device having a six inch diagonal [16]. Thus, it has been evidenced that VM is of interest for application to flat panel displays because of its potential for high image quality, flat format, and low power requirements. However, some key technical challenges still remain: determining suitable phosphors, achieving lower drive voltages, and developing cost effective drive circuitry [17]. A model for field emission flat panel displays that will allow rapid analysis of display performance over a broad variety of design approaches has been developed by Kesling and Hunt [17]. This requires, first, developing an adequate model for a single emission site, then, progressively expanding the model to describe an array of sites forming a single pixel, an array of pixels forming a complete display, and finally the interface circuitry required to drive the display.

The model supplies current-voltage and capacitance characteristics of the electrical elements and the luminance distribution at the anode. The current-voltage characteristics include the effects of grid leakage current. Intermediate quantities such as field strengths, charge densities and electron trajectories are also available.

Figure 4 shows a block diagram of the general approach for determining the desired device characteristics. The approach is suitable for devices with complex geometries and multiple control elements.

The initial analysis considers a simple triode in order to verify the model's performance. Figure 5 shows a small array of such simple triodes. Figure 6 shows a cutaway view of a single simple triode.

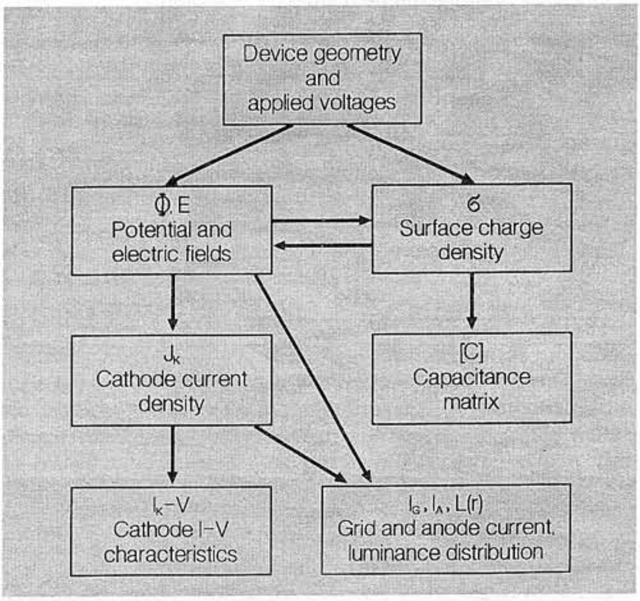

Fig. 4. Approach to find field emitter characteristics. The method uses device geometry and voltages as boundary conditions to find the electronic field in the device. Cathode current density is determined from electric field by the Fowler-Nordheim equation and integrated to give total cathode current as a function of applied voltages. Other currents are determined by tracking electron trajectories (from Ref. [17])

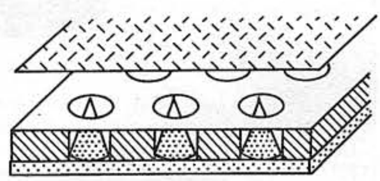

▲ Fig. 5. Small array of simple field emission devices. Gated cathodes with conical cathode bases and hemispherical cathode tips are the simplest device of interest. The phosphor screen acts as an anode to make a triode configuration (from Ref. [17])

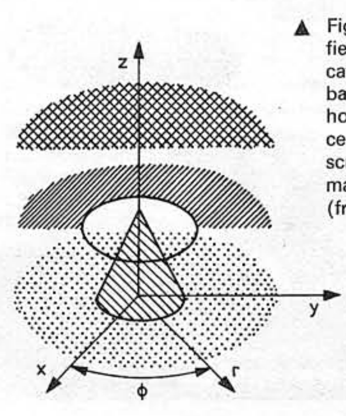

Fig. 6. Cutaway view of a simple triode emission site. Cylindrical symmetry allows two-dimensional modelling in $r-z$ plane (from Ref. [17])

The Fowler-Nordheim equation gives cathode current density from the electric field at the cathode surface. Electron trajectories are computed using a finite difference approximation to solve the non-linear, second-order differential equations of motion in two dimensions. Knowledge of the trajectories allows determination of the grid and anode current densities from the cathode current density. Device currents are determined either by numerical surface integration or by fitting polynomial functions to the current density data and integrating them analytically. The latter approach is particularly suitable at the anode, where it leads to a functional description of the luminance distribution, which is useful for image quality analysis.

The generation of $I-V$ characteristics is greatly simplified by employing superposition of boundary conditions to Laplace's equation. The entire $I-V$ characteristics can be determined with only three sets of field boundary conditions (and hence only three finite element analyses) for a triode. A tetrode requires four, and so on. Screen luminance is related to the anode current density by the phosphor efficiency [17].

4. FEAs display design and construction

A typical pixel cutaway of a thin vacuum-florescent display utilizing a matrix-addressable array of groups of Spindt-type field-emission tips is shown in Figure 7 after Ref. [18].

The emitting surface is built on a baseplate (a 5-in-diameter silicon wafer). Individual pixels are 250-μm on a side each, and contain three color elements. The emitters are addressed in one direction by adjacent stripes of the molybdenum base film 175 μm wide on 250-μm centers, and are addressed in the orthogonal direction by the gate film, which is patterned in adjacent groups of three stripes each 40 μm wide on 66-μm centers, one for each color element of the pixel.

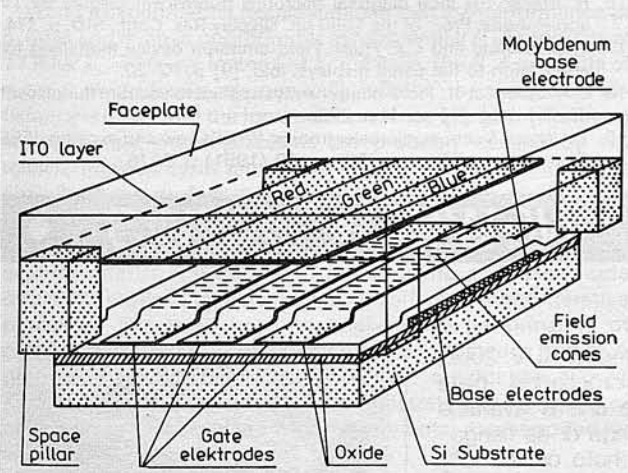

Fig. 7. Typical pixel cutaway of a FEA – FPD (from Ref. [18])

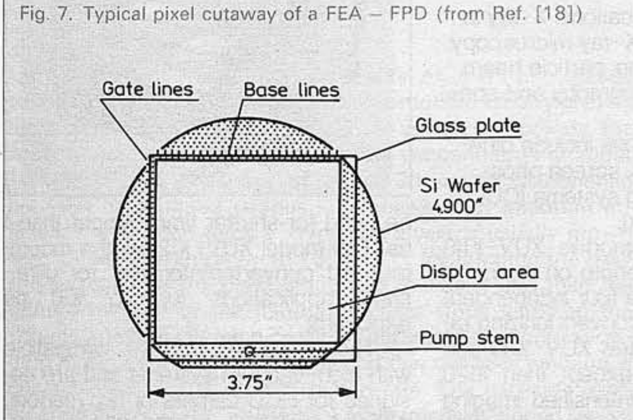

Fig. 8. Display assembly of a FEA – FPD (from Ref. [18])

The complete display (Fig.8) consists of a square array of 338×338 pixels. Contact to the matrix address lines is made at the periphery of the wafer not covered by the pixel array. The faceplate is coated with transparent conducting indium tin oxide (ITO), patterned with stripes of the three colored phosphors, and registered to oppose the corresponding stripes on the gate film. The faceplate is separated from the baseplate by $50 \times 50 \times 75$ μm pillars, which rest on 75-μm-wide stripes between cathode rows. This pillar height allows up to 1000 V to be applied between the screen and cathode without breakdown. The faceplate is larger than the display area to allow for a pumpout strem without interfering with the visible part of the display. The vacuum seal is made along the lines of overlap between the faceplate and the baseplate. The entire device is then connected to a turbomolecular pumped chamber and baked to 125°C for 12 h, after which the pressure in the pumped chamber approaches 10^{-9} torr as measured with an ion gauge.

5. Proximity focusing and addressing in FEAs – FPDs

In discussing these two important problems related to FEAs – FPDs, we will follow the considerations presented by Spindt et al. in Ref. [18]. Let us begin with the proximity focusing problem.

It is necessary to prevent large numbers of electrons from hitting color stripes adjacent to the color phosphor at which they have been aimed. Such „overlap" would give rise to crosstalk. This is accomplished by placing the cathodes in close proximity to the screen. In Spindt's arrangement [18], the electric field between the gate film and the screen is sufficiently large that the space-charge effects are eliminated. Thus, the divergence of the electron beam emerging from a simple tip may be simply calculated. If V_G is the voltage applied to the gate film, and V_S is the voltage applied to the screen, consider an electron emerging from the plane of the gate film with velocity v_G making an angle ϑ with the normal. If t is the transit time, the lateral distance moved by the electron in travelling from gate to screen is

$$\delta = v_G t \sin\vartheta = \left[\frac{2eV_G}{m}\right]^{1/2} t \sin\vartheta \qquad (3)$$

Applying Newton's law in the axial direction gives

$$\left[\frac{V_S - V_G}{d}\right] e = m\ddot{x} \qquad (4)$$

and solving for t gives

$$\delta = 2\frac{(V_G)^{1/2}}{(V_S - V_G)} \sin\vartheta \left[(V_S - V_G \sin^2\vartheta)^{1/2} d \, (V_G)^{1/2} \cos\vartheta\right] d \qquad (5)$$

As an example, if we choose $V_S = 900$ V, $V_G = 100$ V, and a maximum half-angle emission from the tip $\vartheta_m = 30°$ (worst case), (5) gives

$$\delta_m \approx 0.26d \qquad (6)$$

Adjacent color stripes are in contact and are approximately 66 μm wide, whereas the cathode arrays that provide electrons from the color elements are separated by 25 μm, and are only 40 μm wide. This allows for $\delta \leqslant 13$ μm, or $d \leqslant 50$ μm. We note also that the electric field between the gate film and the screen in this case is $800/(75 \cdot 10^{-4}) \approx 10^5$ V/cm. This is approaching the limit at which vacuum breakdown can occur [18].

The phosphors are not aluminized; nevertheless, it has been found that electron energies above 500 V are required before reasonable luminous efficiencies are obtained with the red and blue phosphors. On the other hand, excellent brightness is obtained with green phosphors (ZnO : Zn) at 200 V. Thus, given the size of the color elements, the screen voltage needed for reasonable phosphor brightness, and the onset of vacuum breakdown, the separation distance between the gate film and the screen is constrained to a narrow range.

The problem of addressing in FEAs-FPDs seems to be more complicated [18].

Because of the relatively high capacitance of the stripes of cathodes and the relatively high resistance of the thin molybdenum film, the time constant for application of the full voltage to an individual pixel does not allow individual pixels to be addressed at conventional raster-scan speeds. However, one may use the scanning strategy of sequentially addressing one line at a time in the horizontal direction while simultaneously driving all the base lines in the vertical direction. Even allowing for the rise and fall times, each pixel is on for a much longer time per frame than in a conventional raster scan. The relationship between pixel brightness B and screen voltage, screen current density J, and the fraction of time per frame that a pixel is activated f is given by

$$B = A \cdot \eta (J, V_S) \cdot Jf \quad (7)$$

where $\eta (J, V_S)$ is the conversion efficiency from electron beam energy to light energy, and A is the conversion factor from light energy to brightness, which is dependent on the phosphor color. To obtain comparable brightness in a given situation with a conventional raster scan CRT we note that V_S is reduced by a factor of about 10, but f increased by a factor up to the number of pixels in a line (338). Even allowing some dependence of η on J and V_S, the current density requirements for the cathodes are extremely low.

6. Outlook

In this article, we have reviewed up-dated results on high-resolution, three-color high-brightness vacuum fluorescent display based on the Spindt-type field-emitters. These results indicate that the major assembly and processing problems have been overcome, but that more refinements are necessary before the characteristics of a fully operational large-area display can be ascertained [18]. Among these refinements the key factor required to make VM successful for high-resolution FPDs is closely related to the understanding and control of the physics, materials, and microfabrication technology for FEAs, especially from the viewpoint of optimizing the concept „the most current for the least voltage" [19].

References

1. Vacuum Microelectronics 1988 (eds. H.F. Gray and C.A. Spindt). IEEE Trans. Electron Devices, **ED-36**, no. 11. pt II (1989) p. 2635.
2. Vacuum Microelectronics 1989 (ed. R.E. Turner). Inst. Phys. Conf. Ser., no. 99, A. Hilger, IOP Publ., Bristol 1989.
3. Vacuum Microelectronics 1990 (eds. E.A. Adler, C.A. Spindt and H.F. Gray). IEEE Trans. Electron Devices, **ED-38**, no. 10 (1991) p. 2275
4. Proceedings of the 4th (1991, Nagahama, Japan) and 5th (1992, Vienna, Austria) Vacuum Microelectronics Conferences will be published in J.Vac. Sci. Technol., ser. B, 1992 and 1993, respectively.
5. *H.F. Gray, G.J. Campisi* and *R. F. Greene*: A vacuum field effect transistor using Si emitter arrays. Proc. Int. Electron Devices Meeting, Los Angeles, December 1986.
6. *M.A. Herman*: Vacuum Microelectronics — present status and development trends. Proc. Int. Conf. „Microelectronics 92", Warsaw, September 1992. SPIE Conf. Proc. Ser., **WA 92** (1992).
7. *K.E. Petersen*: Silicon as a mechanical material. Proc. IEEE, **70** (1982) p. 420.
8. *T.S. Ravi, R.B. Marcus* and *D. Liu*: Oxidation sharpening of silicon tips. J. Vac. Sci. Technol., **B9** (1991) p. 2733.
9. *D. Stephani* et al.: Fabrication of field-emitter arrays with 0.4 μm grid apertures. Abstracts of the 5th Int. Vacuum Microelectronics Conf. 1992, Vienna, Austria, p. 8–4.
10. *C.A. Spindt* et al.: Field-emitter arrays for vacuum microelectronics. IEEE Trans. Electron Devices, **ED**-38, no. 10 (1991) p. 2355.
11. *I. Brodie*: Physical considerations in vacuum microelectronic devices. IEEE Trans. Electron Devices, **ED-36**, no. 11, pt II (1989) p. 2641.
12. *R.H. Fowler* and *L. Nordheim*: Electron emission in intense electric field. Proc. Royal Soc. London, ser A, **119** (1928) p. 173.
13. *P.H. Cutler* et al.: Tunneling theory and vacuum microelectronics. ibid. [2] p. 121.
14. *C.A. Spindt* et al.: Physical properties of thin-film field emission cathodes with molybdenum cones. J. Appl Phys., **47** (1976) p. 5248.
15. *R. Meyer* et al.: Microtips fluorescent displays. Japan Display 1986, p. 512.
16. *R. Meyer*: Six inch diagonal microtips fluorescent display for TV applications. Proc. of the 1990 Int. Display Res. Conf., SID, p. 374.
17. *W.D. Kesling* and *C.E. Hunt*: Field-emission device modelling for application to flat panel displays. ibid. [9] p. P2-20.
18. *C.A. Spindt* et al.: Field-emitter arrays applied to vacuum fluorescent display. ibid. [1] no. 1, p. 225.
19. *T. Utsumi*: Vacuum microelectronics: What's new and exciting. IEEE Trans. Electron Devices, **38**, no. 10 (1991) p. 2276.